J. theor. Biol. (2001) **212,** 111–125
doi:10.1006/jtbi.2001.2362, available online at http://www.idealibrary.com on IDEAL®

Stochastic Effects in Intercellular Calcium Spiking in Hepatocytes

M. E. Gracheva*‡, R. Toral† and J. D. Gunton*

**Department of Physics, Lehigh University, Bethlehem, PA* 18015 *and †Instituto Mediterraneo de Estudios Avanzados, CSIC-UIB, E*-07071 *Palma de Mallorca, Spain*

(*Received on* 21 *January* 2001, *Accepted in revised form on* 25 *May* 2001)

We carry out a Monte Carlo simulation of stochastic effects for two models of intercellular calcium wave propagation in rat hepatocytes. Both models involve gap junction diffusion by a second messenger. We find that, in general, the stochastic effects improve agreement with experiment, for a reasonable choice of model parameters. Both stochastic models exhibit baseline fluctuations and variations in the peak heights of Ca^{2+}. In addition, we find for one model that there is a distribution of latency times, rather than a single latency time, with a distribution width which is comparable to the experimental observation of spike widths. We also find for the other model with low gap junction diffusion that it is possible for cell multiplets to oscillate independently initially, but to subsequently become synchronized.

1. Introduction

Cell-to-cell signals control the development of multicellular organisms as well as most of their functions (Goldbeter, 1996). Calcium signaling plays a particularly important role in cell communication. Single hepatocytes respond to hormonal stimulation with repetitive spikes in intracellular Ca^{2+} concentration (Thomas *et al.*, 1991, 1995, 1996). Multiplets of hepatocytes can exhibit well-coordinated spiking, known as intercellular Ca^{2+} waves. Such intercellular communication can take different forms, including gap junction coupling, paracrine signaling and the recently discovered extracellular calcium signaling (Höfer *et al.*, 2000). In particular, the diffusion of second messengers through gap junctions appears to be responsible for intercellular calcium waves in tracheal ciliated cells (Sneyd *et al.*, 1995; Sanderson *et al.*, 1990), glial cells (Charles *et al.*, 1992), pancreatic acinar cells (Loessberg-Stauffer *et al.*, 1993; Yule *et al.*, 1996) and other types (Sanderson *et al.*, 1994).

There exist two different types of experimental studies of such waves. In one class, a single cell of a cultured monolayer is stimulated mechanically, inducing the propagation of Ca^{2+} waves in the adjacent cells. Such studies have been carried out on tracheal epithelial cells (Hansen *et al.*, 1993) and endothelial cells. Sneyd *et al.* (1995, 1998) have proposed a model for these intercellular waves, which assumes gap junctional diffusion of IP_3 between adjacent cells. Mechanical stimulation of a single cell produces IP_3 within the cell, which in turn causes the release of Ca^{2+} from internal stores in the form of an intracellular Ca^{2+} wave. Diffusion of IP_3 between cells then initiates calcium waves in adjacent cells. This process continues as long as the amount of IP_3 entering a given cell is sufficient to induce a Ca^{2+} wave. In another class of experiments, studies are carried out on freshly isolated systems of connected cells that are globally stimulated

‡Author to whom correspondence should be addressed.

0022–5193/01/170111 + 15 $35.00/0

by hormones (Loessberg-Stauffer *et al.*, 1993; Nathanson *et al.*, 1992; Combettes *et al.*, 1994; Nathanson *et al.*, 1995; Robb-Gaspers & Thomas, 1995). An interesting feature of these studies for liver cells (which are tightly coupled by gap junctions) is the sequential pattern of Ca^{2+} spiking in the different connected cells, which creates the appearance of Ca^{2+} waves (Nicholson *et al.*, 1987).

Some recent papers have studied the mechanisms that control the coordination and intercellular propagation of calcium waves induced in rat hepatocytes (studying propagation of such intercellular Ca^{2+} waves in doublet and triplet cells). A first paper by Tordjmann *et al.* (1997) studied calcium waves induced by noradrenaline and showed that gap junction coupling is necessary for the coordination of the oscillations between the different cells. The authors also demonstrated that it is necessary to have hormone stimulation at each hepatocyte in order to have cell–cell calcium signal propagation. Furthermore, they also found that there were functional differences between adjacent hepatocytes. A subsequent paper by the same authors (Tordjmann *et al.*, 1998) continued these studies, combining single-cell studies with experiments on cell populations isolated from the peripheral (periportal) and central (perivenous) zones of the liver cell plate. They found strong evidence that the sequential pattern of calcium responses to vasopressin in these multicellular rat hepatocyte systems was due to a gradient of cell sensitivity (from cell to cell) for the hormone. The first cell to respond had the greatest sensitivity to the global stimulus, while the last cell to respond had the least sensitivity. This is an important result, since such gradients may impose an orientation on calcium waves in liver cells and provide a pacemaker-like mechanism for regulating intercellular communication in the liver. Based upon these experimental studies, two models have been put forward in order to explain the observed results.

The first model is due to Dupont *et al.* (2000) who studied a model based on junctional coupling of multiple hepatocytes which differ in their sensitivity to the hormonal stimulus. As a consequence of this difference, the intrinsic frequency of intracellular calcium oscillations also varies from cell to cell. These oscillators are coupled by an intercellular messenger, which could be either Ca^{2+} or inositol 1,4,5-trisphosphate IP_3. The model yielded intercellular waves that were confirmed experimentally (Dupont *et al.*, 2000). The authors also presented experimental evidence that the degree of synchronization is greater for the first few spikes, in agreement with the prediction of their model. They also presented evidence that suggested, within the context of their model, that IP_3 diffusion through gap junctions (rather than Ca^{2+} diffusion) plays the dominant role in the synchronization of intercellular spiking.

An alternative model has also been proposed by Höfer (1999) to explain the experimental results obtained in the first paper by Tordjmann *et al.* (1997). Höfer noted that this experiment revealed a rather large variability in oscillator frequency between adjacent cells, which he argued is likely to be of random nature. As a consequence he studied the possibility that this originates from random variations in the structural properties of cells (cell size, cell shape, or ER content). In addition, Ca^{2+} was assumed to be the second messenger (Höfer, 1999). His results were in reasonable agreement with those of Tordjmann *et al.* (1997).

Although we are not in a position to judge the relative merits of the two models, both are relatively successful and quite interesting. However, they both have limitations. For example, the calcium spikes in the Dupont *et al.* (2000) model are extremely sharp, whereas the experimental spikes are broader. Höfer's model predicts more reasonable spike widths, but predicts an intercellular synchronization at low stimulus that seems inconsistent with experiment (cf. Section 2). In addition, both models are deterministic, described by differential equations with boundary conditions for the cell multiplets and with diffusion between cells. Such models, however, do not produce stochastic effects such as fluctuations in the baseline values of calcium and variations in the amplitudes and widths of the spikes that have been seen experimentally (Tordjmann *et al.*, 1997, 1998). Indeed, since the number densities of intracellular signaling molecules are typically low of order $1–10^2\ \mu m^{-3}$, one would expect stochastic effects to be important (Stundzia & Lumsden, 1996; Kraus *et al.*, 1996). To obtain a better explanation of the experimental results, we have

therefore studied stochastic versions of the above two models. Our simulation is based on a Monte Carlo method due to Gillespie (1976, 1977). Stochastic models of intracellular Ca^{2+} spiking for a variety of cell types have been studied previously (Kraus *et al*., 1996; Prank *et al*., 1998; Keizer & Smith, 1998; Keizer *et al*., 1998; Falcke *et al*., 2000).

The outline of our paper is as follows. In Section 2 we define and study a stochastic version of Höfer's model. In Section 3 we study a stochastic version of the Dupont *et al.* model. In both sections, we compare our results with those of the experiment. Finally, in Section 4, we present a brief conclusion.

2. Calcium Synchronization of Heterogeneous Cells

We first study a stochastic version of the deterministic model proposed by Höfer (1999) to explain the synchronization of calcium oscillations in heterogeneous hepatocyte cells found by Tordjmann *et al.* (1997). His model of intracellular dynamics is similar to earlier models (Somogyi & Stucki, 1991; Dupont & Goldbeter, 1993), but includes calcium inhibition of receptors (Bezprozvanny & Ehrlich, 1995; DeYoung & Keizer, 1991). As noted above, he assumed that the rather large variability in intrinsic oscillator frequencies observed by Tordjmann *et al.* is due to random heterogeneities of structural properties (such as cell size, cell shape and ER content). He also argued that since there seems to be no feedback of calcium on PLC in hepatocytes (Bird *et al*., 1997) and since non-metabolizable analogues of IP_3 can also produce calcium oscillations (Thomas *et al*., 1991), IP_3 fluctuations are not needed to produce calcium oscillations. He thus assumed that the concentration of IP_3 rapidly reaches a steady-state value (which can differ for different cells) that is treated as a parameter of the model. In addition, he argued that since calcium oscillations may cause continuously changing junctional fluxes of calcium, the intercellular synchronization might be due to a Ca^{2+} flux across cellular gap junctions. The Höfer model (1999) considers a series of $j = 1, 2, \ldots, N$ linearly connected cells. We will be considering in this study single cells, $N = 1$, doublets, $N = 2$ and triplets, $N = 3$. Let x_j and y_j be, respectively, the average cytosolic calcium concentration and the average free calcium concentration in the ER in cell j, and define $z_j = x_j + (C_{ER}^j/C_C^j)\, y_j$, where z_j is a measure of the free calcium content in the cell. Here $C_C^j = V_C^j(1 + B_0/K_B)$ and $C_{ER}^j = V_{ER}^j (1 + B_0/K_B)$ are effective volumes of the cytosol and endoplasmic reticulum of cell j, respectively. (These arise in the model from a quasi-steady-state approximation for calcium buffering). V_C^j and V_{ER}^j are the real volumes of the cytosol and ER, and K_B and B_0 are a dissociation constant and the total concentration of calcium binding sites, respectively. Höfer estimates that this cytosolic calcium buffering factor $(1 + B_0/K_B)$ ranges from 20 to 100 or so depending on cell type and chooses it as 75 in his calculation.

After some simplification Höfer (1999) obtained the following deterministic model for the time evolution of the x_j and z_j variables in the case of a doublet, $N = 2$:

$$\frac{dx_j}{dt} = \rho_j \left(v_0 + v_c \frac{P_j}{K_0 + P_j} - v_4 \frac{x_j^2}{K_4^2 + x_j^2} + \frac{\alpha_j k_r(x_j, P_j)}{\beta_j} (z_j - (1 + \beta_j) x_j) - \alpha_j v_3 \frac{x_j^2}{K_3^2 + x_j^2} \right) + \gamma(x_i - x_j), \tag{1}$$

$$\frac{dz_j}{dt} = \rho_j \left(v_0 + v_c \frac{P_j}{K_0 + P_j} - v_4 \frac{x_j^2}{K_4^2 + x_j^2} \right) + \gamma(x_i - x_j). \tag{2}$$

The last term, proportional to γ, denotes diffusion between cells. γ is a junctional coupling coefficient and is proportional to the gap-junctional permeability, but we will refer to it as to the gap-junctional permeability coefficient. The index pairs $(i, j) = (1, 2)$ and $(2, 1)$. The system can be easily generated to the case of more than two cells. In these equations P_j is the IP_3 concentration in cell j. The IP_3R release function $k_r(x_j, P_j)$ describes the gating kinetics of the IP_3 receptor

R and is given by

$$k_r(x_j, P_j) = k_1\left[\frac{d_2(d_1+P_j)P_j x_j}{(d_p+P_j)(d_a+x_j)(d_2(d_1+P_j)+x_j(d_3+P_j))}\right]^3 + k_2\,, \tag{3}$$

an expression based on earlier theoretical work (DeYoung & Keizer, 1991; Li & Rinzel, 1994). The parameters $\rho_j = A^j_{PM}/C^j_C$, $\alpha_j = A^j_{ER}/A^j_{PM}$ and $\beta_j = C^j_{ER}/C^j_C$ define various structural characteristics of the j-th cell and account for the heterogeneous behavior of different cells. The variables A^j_{ER} and A^j_{PM} are the areas of the ER and plasma membrane of cell j, respectively. The parameter v_0 describes a calcium leakage from the background, v_c is the maximum rate of IP_3-induced calcium formation (influx), v_3 is the maximum rate of ER uptake of calcium from the cytosol and v_4 is the maximum rate of calcium extrusion through the plasma membrane.The definitions of the other parameters as well as their values are given in Höfer (1999). Table 1 summarizes the values we adopt for these parameters in the present paper. Note that the parameters A_{PM}, C_C, A_{ER}, B_0 and K_B are not given, as they only appear in ratios in the model.

The above set of Höfer's equations is deterministic and completely ignores the fluctuations that appear from the fact that the chemical reactions do not occur uniformly and continuously in time. Gillespie's method (Gillespie, 1976) considers specifically that (a) the concentration of molecular species can only vary by a discrete amount and (b) the chemical reaction itself is a stochastic process that occurs with a certain rate. Therefore, it is not possible to determine which reaction will occur next, but rather what is the probability that a given reaction will take place.

In accordance with Gillespie's method, we introduce the number of calcium ions in the cytosol of cell j as X_j (the calcium ion "population number") and correspondingly the population number Z_j of calcium ions, such that the concentrations of the reactants are obtained as

$$x_j = \frac{X_j}{\Omega}, \quad z_j = \frac{Z_j}{\Omega}. \tag{4}$$

TABLE 1

Typical simulation constants for model with intercellular diffusion of Ca^{2+}: P is IP_3 concentration, v_0 is a background Ca^{2+} leakage, v_c is max rate of IP_3 induced Ca^{2+} influx, v_3 is max rate of ER uptake of Ca^{2+}, v_4 is max rate of calcium efflux, other parameters see (*Höfer*, 1999)

Parameter	Value
P	2.0 μM
v_0	0.2 μM/s
v_c	4.0 μM/s
v_3	9.0 μM/s
v_4	3.6 μM/s
K_0	4.0 μM
K_3	0.12 μM
K_4	0.12 μM
d_1	0.3 μM
d_2	0.4 μM
d_3	0.2 μM
d_p	0.2 μM
d_a	0.4 μM
k_1	40.0 s^{-1}
k_2	0.02 s^{-1}
ρ	0.02 μm^{-1}
α	2.0
β	0.1

In this model Ω is the volume of the cytosolic compartment of the cell, with fluctuation effects being most notable for small Ω. The population numbers X_j and Z_j can vary by discrete, integer, amounts according to some probability that reflects the possible reactions taking place in the system. The possible events and their reaction constants are defined in Table 2. Given eqns (1)–(3) we choose the following expressions for the rates:

$$a^{(1)}_j = \Omega\rho_j\left(v_0 + v_c\frac{P_j}{K_0+P_j} + \frac{\alpha_j k_r(x_j, P_j)}{\beta_j} z_j\right), \tag{5}$$

$$a^{(2)}_j = \Omega\rho_j\left(v_4\frac{x_j^2}{K_4^2+x_j^2} + \frac{\alpha_j k_r(x_j, P_j)}{\beta_j}(1+\beta_j x_j) + \alpha_j v_3\frac{x_j^2}{K_3^2+x_j^2}\right), \tag{6}$$

$$a^{(3)}_j = \Omega\rho_j\left(v_0 + v_c\frac{P_j}{K_0+P_j}\right), \tag{7}$$

TABLE 2
Stochastic formulation of model with intercellular diffusion of Ca^{2+}

Reaction constant	Stochastic process
$a_j^{(1)}$	$X_j \to X_j + 1$
$a_j^{(2)}$	$X_j \to X_j - 1$
$a_j^{(3)}$	$Z_j \to Z_j + 1$
$a_j^{(4)}$	$Z_j \to Z_j - 1$
$a_j^{(5)}$	$X_j \to X_j + 1$
	$X_{j+1} \to X_{j+1} - 1$
$a_j^{(6)}$	$X_j \to X_j - 1$
	$X_{j+1} \to X_{j+1} + 1$
$a_j^{(7)}$	$Z_j \to Z_j + 1$
	$Z_{j+1} \to Z_{j+1} - 1$
$a_j^{(8)}$	$Z_j \to Z_j - 1$
	$Z_{j+1} \to Z_{j+1} + 1$

$$a_j^{(4)} = \Omega \rho_j v_4 \frac{x_j^2}{K_4^2 + x_j^2}, \tag{8}$$

$$a_j^{(5)} = \gamma_{max}(X_{j+1} - X_j, 0), \tag{9}$$

$$a_j^{(6)} = \gamma_{max}(X_j - X_{j+1}, 0), \tag{10}$$

$$a_j^{(7)} = \gamma_{max}(X_{j+1} - X_j, 0), \tag{11}$$

$$a_j^{(8)} = \gamma_{max}(X_j - X_{j+1}, 0) \tag{12}$$

and the convention that, whenever they appear, we define $X_0 = Z_0 = 0, X_{N+1} = Z_{N+1} = 0$ as the boundary condition for diffusion. Equations (5)–(8) describe the intracellular calcium dynamics while eqns (9)–(12) describe gap junction diffusion. The stochastic simulation proceeds (Gillespie, 1977) by choosing randomly one of the $8 \times N$ events with a probability proportional to the reaction rate, where N is the number of connected cells. Once the event is selected, the number populations change accordingly and time increases by a given amount.

Following (Höfer, 1999) we consider a spherical cell with a radius of 6 μm, with a cell volume of about 900 μm^3, one third of which is a cytosolic volume of about 300 μm^3. We have considered Ω to be essentially a parameter controlling the size of the fluctuations. We display our results for $\Omega = 300$ μm^3, i.e. the cytosolic cell volume. Fig. 1 shows the calcium oscillations for one isolated cell in our stochastic model for $\Omega = 300$ and 10^5, respectively. Note that the result for large $\Omega = 10^5$ agrees with the deterministic limit (Höfer, 1999).

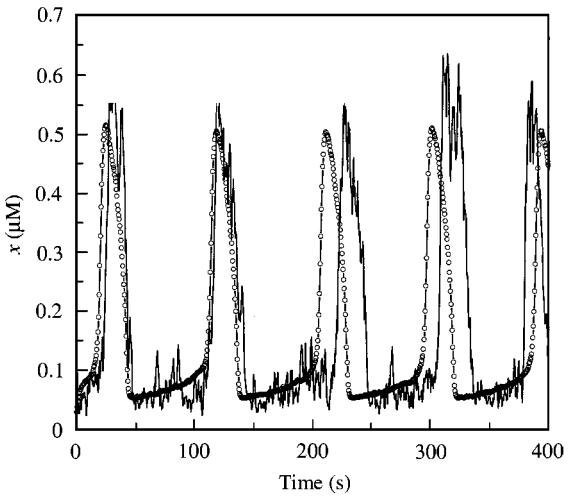

FIG. 1. Calcium oscillations in the stochastic version of Höfer's model for a single cell, eqn (1) with $N = 1$ and $\gamma = 0$, for different values of the cytosolic volume $\Omega = 300$ μm^3, 10^5 μm^3. We observe that a smooth behavior, corresponding to the deterministic limit, is already achieved for $\Omega = 10^5$. Parameter values are as listed in Table 1, with $\beta = 0.1$, $P = 2.0$ μM and $\rho = 0.02$. We have taken as initial condition for the cell the resting state without agonist, $P = 0$ μM. (——) Omega = 300; (—∘—) Omega = 100000.

We have not found a value in the literature for the cell–cell permeability γ that enters in the gap junction coupling. Therefore, we will follow (Höfer, 1999) and study the calcium oscillations for a range of permeability values. To determine the maximum value of γ that we should use in the stochastic model, we simulated the experimental study (Tordjmann *et al.*, 1997) of the doublet of hepatocytes. In the experiment (Tordjmann *et al.*, 1997), the authors first stimulated only one of the cells in the doublet with a hormonal input (local perfusion). They then stimulated both cells simultaneously (global perfusion). From these studies they found that local perfusion does not produce spiking in the second (unstimulated) cell. Global perfusion of both cells, on the other hand, produces well-synchronized Ca^{2+} oscillations in the two cells. We thus use this to fix our gap junction permeability coefficient, such that stimulation of only one cell in the doublet does not produce

oscillations in the second (unstimulated) cell for a given permeability coefficient between cells. In Fig. 2a–c we show our results of stimulating only one cell in the doublet. We increase the cell–cell permeability to find the largest value that will not produce Ca^{2+} spiking in the second cell. We see that the two cells respond differently, with different periods of oscillations; in neither case does the unstimulated cell show Ca^{2+} oscillations. However, if we stimulate both hepatocytes they respond with well-coordinated Ca^{2+} oscillations. This yields the value of $\gamma_{max} = 0.07\ s^{-1}$, which is in the range of values used by Höfer (1999).

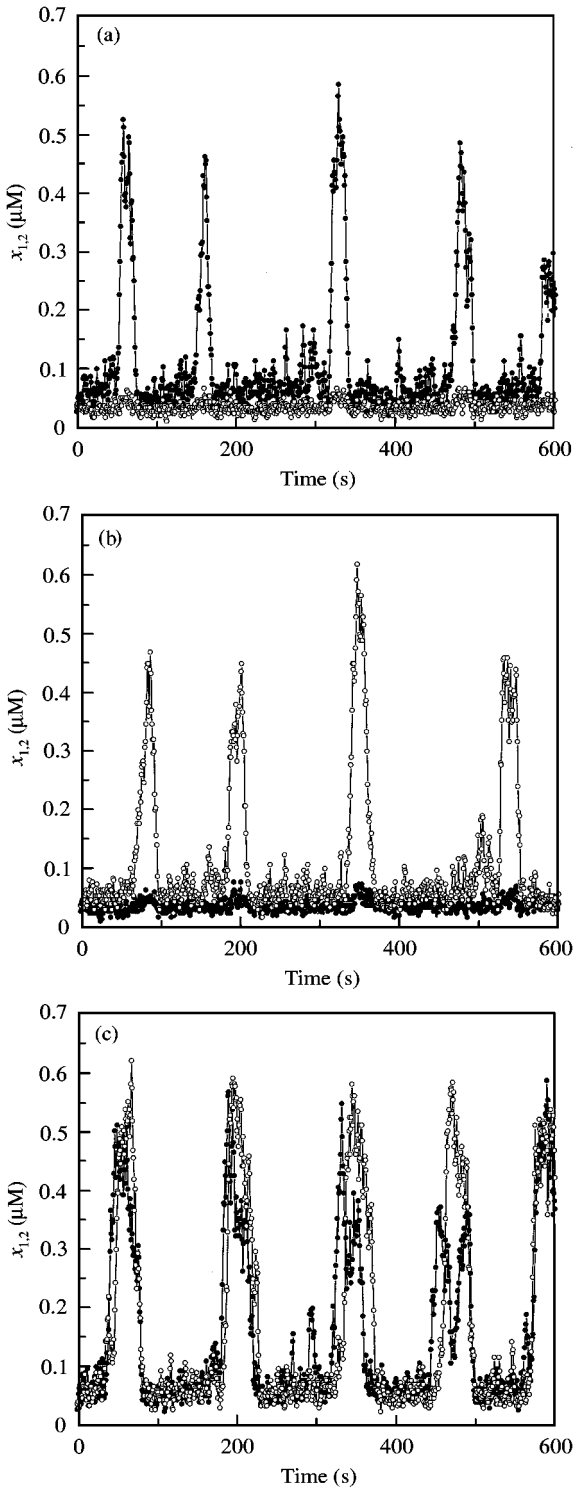

Next we study the behavior of two connected hepatocytes which are globally stimulated. To simulate the experimental situation of two slightly different cells, we choose different structural parameters, with $\beta_1 = 0.15, \beta_2 = 0.2$. We do not follow Höfer in our choice of structural parameters since for his choice of parameters ($\beta_1 = 0.1, \beta_2 = 0.2$) for a given volume $\Omega = 300$ we could not obtain a well-synchronized response from two coupled cells. We also choose slightly different values of ρ (than Höfer) to have better synchronized oscillation patterns. The results of the simulation are shown in Figs. 3a–c for $\gamma = 0.0$ and $0.07\ s^{-1}$. The calcium oscillations in the two cells are totally uncoordinated if the membrane permeability is set to zero, as should be the case Fig. 3(a). For a value of the permeability $\gamma = 0.07\ s^{-1}$ we find 1:1 locking (Fig. 3b). Fig. 3c shows the result for $\gamma = 0.07\ s^{-1}$ in the deterministic limit of large Ω, which is in agreement with Höfer's results for this choice of parameters.

We have also simulated the experimental situation in which, after a few coordinated oscillations, the membrane permeability between cells is blocked in the interval between 200 and 500 s in such a way as to prevent Ca^{2+} from passing through the membrane (γ is set to zero in

FIG. 2. Calcium spiking in the stochastic version of Höfer's model including diffusion of Ca^{2+} through gap junctions for $N = 2$ connected cells. Solid symbols correspond to variable x_1 and empty symbols to x_2 (the lines are a guide to the eye). Values of the parameters are as in Table 1 with $\beta_1 = 0.2$, $\beta_2 = 0.12$, $\rho_1 = \rho_2 = 0.015$, $\gamma = 0.07\ s^{-1}$, $\Omega = 300\ \mu m^3$. In (a) only the first cell is stimulated with agonist: $P_1 = 2\ \mu M$, $P_2 = 0\ \mu M$, while in (b) only the second cell is stimulated with agonist: $P_1 = 0\ \mu M$, $P_2 = 2\ \mu M$. In (c) both cells are globally stimulated with agonist: $P_1 = P_2 = 2\ \mu M$. The initial condition for both cells is the resting state without agonist ($P_1 = P_2 = 0\ \mu M$). The figure shows that, for permeability constant less than $\gamma = 0.07\ s^{-1}$, unstimulated cells in doublet do not produce calcium oscillations, but when both cells are stimulated they produce well-coordinated spikes.

the model). In this case the cells lose synchronization, but after washing the chemical responsible for the blocking at $t = 500$ s, the cells regain synchronization. This behavior is clearly seen in Fig. 4a. The stochastic model yields a variation in the amplitude of oscillations and fluctuations in the baseline value of Ca^{2+}, in agreement with the experimental results (Tordjmann *et al.*, 1998). These effects are absent in the deterministic limit of the model, shown in Fig. 4b.

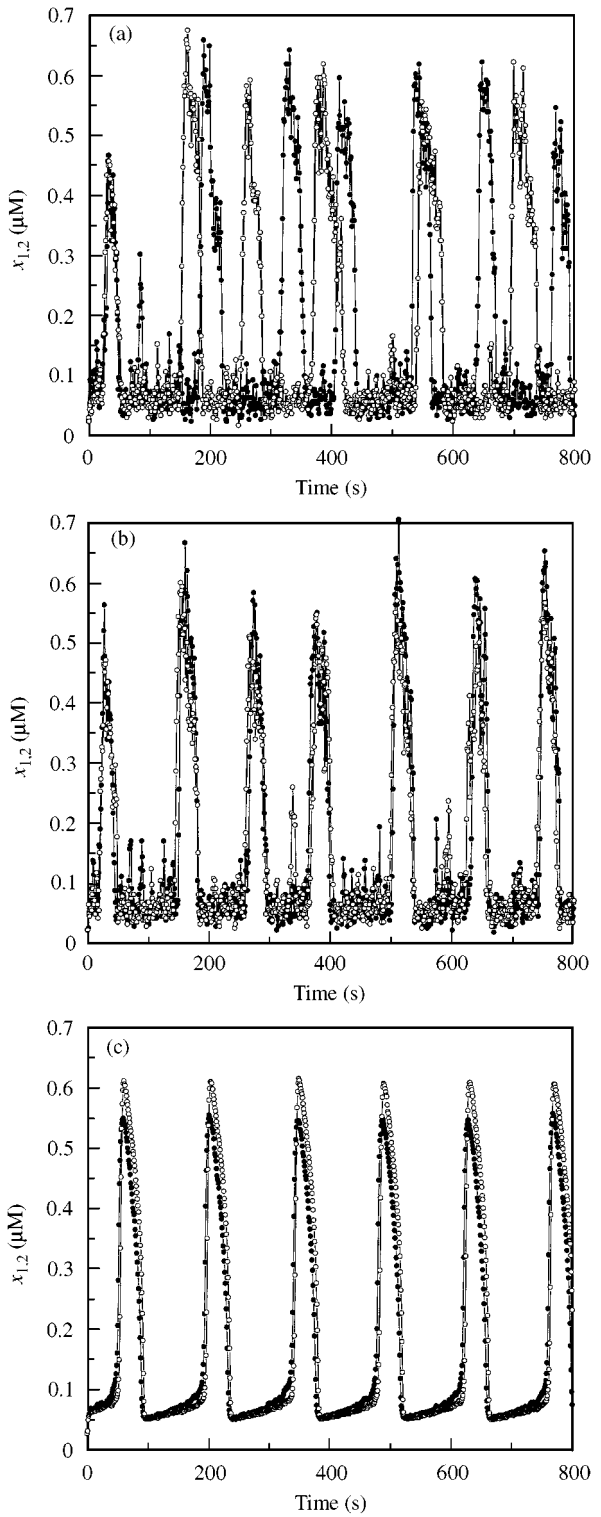

Finally, we model the experimental study of a triplet of hepatocytes, in which one can see synchronized intercellular signaling. However, if a heparin treatment is applied to the intermediate cell the calcium oscillations of the middle cell are altered. In addition, the synchronized spiking between the first and third cells is destroyed. Fig. 5a show the results of our simulation. It can be seen that after the heparin application at $t = 200$ s [parameters $k_1 = 0.0$ in eqn (3) and $v_c = 0.0$ in eqn (1)] there are no calcium oscillations in the second cell, and the first and third cells in the triplet spike asynchronously. These results are in good agreement with the experimental results (Tordjmann *et al.*, 1998). We also show the results of going to the deterministic limit of large cell volume in Fig. 5b, which are in agreement with the original study, as expected.

The result of simulation of a cell triplet with the membrane permeability between cells set to zero is presented in Fig. 6. It can be clearly seen that cells that are not connected by gap junctions exhibit uncoordinated calcium signaling.

Experiments also show the absence of coordination among the calcium signals in connected hepatocytes at low concentrations of stimuli. The cells respond in an asynchronous fashion because the relative differences in the levels of IP_3 are important. To simulate this situation we have conducted the following numerical experiment. First we applied a low stimulation level $P = 1$ μM to all three cells in the triplet, taking

FIG. 3. Calcium oscillations in the stochastic version of Höfer's model for a doublet $N = 2$ in eqn (1), of globally stimulated cells. Values of parameters are as in Table 1 with $\rho_1 = \rho_2 = 0.02$, $\beta_1 = 0.15$, $\beta_2 = 0.2$, $P_1 = P_2 = 2.0$ and the cell volume is $\Omega = 300\ \mu m^3$. Solid symbols correspond to variable x_1 and empty symbols to x_2 (the lines are a guide to the eye). In (a) the membrane permeability is $\gamma = 0\ s^{-1}$ and the calcium oscillations in the cells are completely uncorrelated. In (b) we use a value of the permeability $\gamma = 0.07\ s^{-1}$ for which there is a 1 : 1 locking in the oscillations of the two cells. Finally, in (c) we show the equivalent locking in the calcium oscillations of the two cells in the deterministic limit obtained for $\Omega = 10^5$ and $\gamma = 0.07\ s^{-1}$.

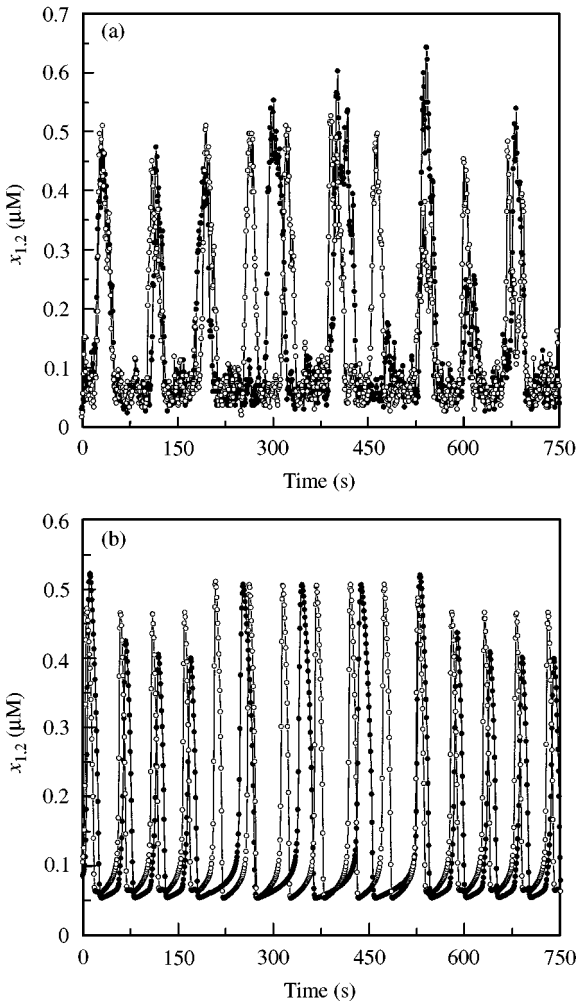

FIG. 4. Effect of the temporal blocking of gap junction between two globally stimulated connected cells in the stochastic version of Höfer's model. Values of the parameters as in Table 1 with $\rho_1 = 0.015$, $\rho_2 = 0.02$, $\beta_1 = \beta_2 = 0.1$, and $P_1 = P_2 = 2.0$. The membrane permeability is $\gamma = 0.06\,s^{-1}$ but it is set to $\gamma = 0\,s^{-1}$ in the time interval $t \in (200\text{–}500)$ s. Solid symbols correspond to variable x_1 and empty symbols to x_2 (the lines are a guide to the eye). In (a) we take $\Omega = 300\ \mu m^3$, while in (b) we consider the deterministic limit achieved with $\Omega = 10^5$ (this is the analog of Fig. 6(a) from (Höfer, 1999)). In both cases (a) and (b) one can see that the cells are initially synchronized from time 0–200 s, but become unsynchronized from 200 to 500 s when there is no coupling between the two cells. They regain synchronization for times greater than 500 s. In the stochastic case (a) there are fluctuations in the baseline value of Ca^{2+} concentration and in the amplitude of the oscillations, in accordance with the experimental results of Tordjmann *et al.* (1998). These fluctuations are absent in the deterministic model (b).

into account the fact that cells can vary in structural properties (with $\rho_1 = 0.025$, $\rho_2 = 0.015$, and $\rho_3 = 0.02$). Note that the three cells become synchronized for times greater than 600 s (Fig. 7a). This continues to be the case even for membrane permeability constants as small as $\gamma = 0.03$ (result not shown). This behavior has not been seen experimentally. Next, we introduce a gradient in the IP_3 concentration, with $P_1 = 1.2$, $P_2 = 1.1$ and $P_3 = 1.0$, for three structurally identical cells with $\rho_1 = \rho_2 = \rho_3 = 0.02$. Fig. 7b shows that calcium oscillations that are initially synchronous become asynchronous with time due to noise, and then again become synchronous. Although this effect has not been seen experimentally, it would be very interesting to have experimental observations of calcium oscillations over long time intervals for medium stimulation levels, since it is possible that even cells that are initially unsynchronized may become synchronized later on.

3. IP_3 Synchronization via Hormonal Sensitivity Gradient

The second model we study is due to Dupont *et al.* (2000) and considers IP_3 as the second messenger responsible for coordination of Ca^{2+} signaling in connected hepatocytes. This model is based on the experimental observation that the number of external receptors on a hepatocyte membrane depends on its location in the liver cell plate (Tordjmann *et al.*, 1998). Thus the authors consider a model of a multiplet of gap junction connected cells, with a small variation in the individual cell frequencies. The dynamics of each cell j is described by a set of three dynamical variables R_j^{des}, x_j and y_j. These are the fraction of inactive IP_3 receptors, the concentration of cytosolic Ca^{2+} and the concentration of IP_3, respectively. The equations of motion are taken to be

$$\frac{\partial R_j^{des}}{\partial t} = k_+ x_j^4 \frac{1 - R_j^{des}}{1 + (x_j/K_{act})^3} - k_- R_{des}, \qquad (13)$$

$$\frac{\partial x_j}{\partial t} = k_1(b + IR_a)\,[\mathrm{Ca}_{tot} - x_j(\alpha + 1)]$$

$$- V_{MP} \frac{{x_j}^2}{x_j^2 + K_P^2} + D_{\mathrm{Ca}} \frac{\partial^2 x_j}{\partial s^2}, \qquad (14)$$

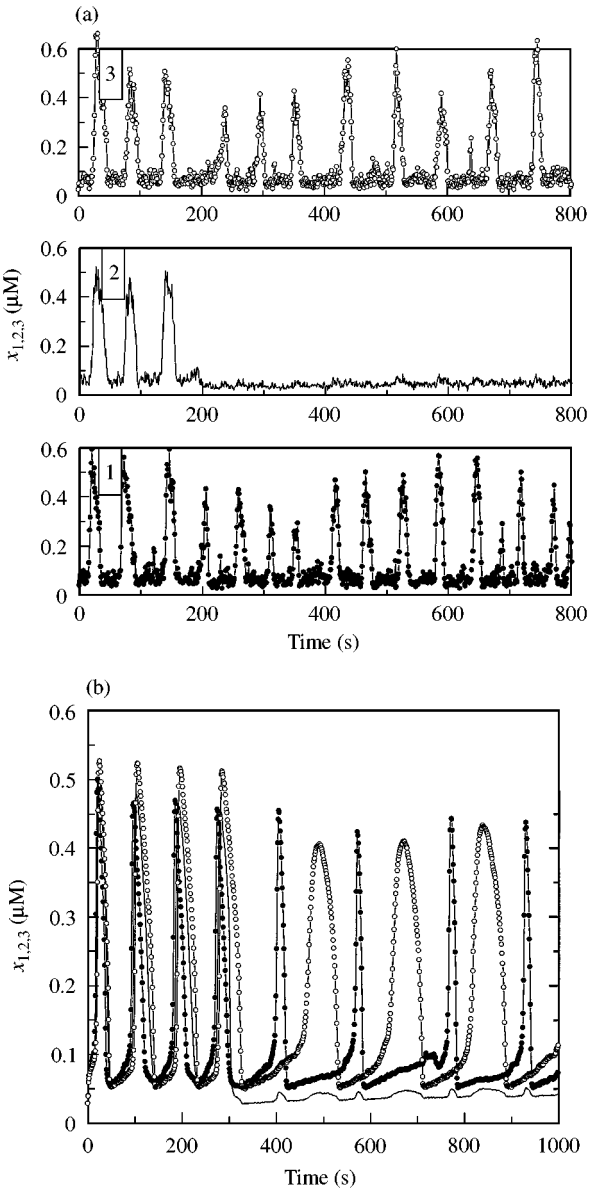

FIG. 5. Simulation of heparin treatment in the stochastic version of Höfer's model for a triplet, $N = 3$ in eqn (1) and (2), of globally stimulated cells. The treatment acts on the middle cell and starts at time $t = 200$ s. It has been simulated by setting $k_1 = 0$ in eqn (3) and $v_c = 0$ in eqn (1) for the second cell, $j = 2$, after $t = 200$ s. We have used the following parameters: $P_1 = P_2 = P_3 = 2$ μM, $\rho_1 = 0.025$, $\rho_2 = 0.018$, $\rho_3 = 0.02$, $\beta_1 = \beta_2 = \beta_3 = 0.1$, $\gamma = 0.07\ s^{-1}$. We plot the time series of the variables x_1, x_2 and x_3 in the cases (a) $\Omega = 300\ \mu m^3$ where stochastic effects are important, and (b) in the deterministic limit with $\Omega = 10^5$, analog of Fig. 6(b) from (Höfer, 1999), where treatment starts at time $t = 300$ s. In both cases, after starting the treatment, there are no oscillations in the second cell and those of the first and the third cell are uncorrelated: (—•—) 1; (——) 2; (—○—) 3.

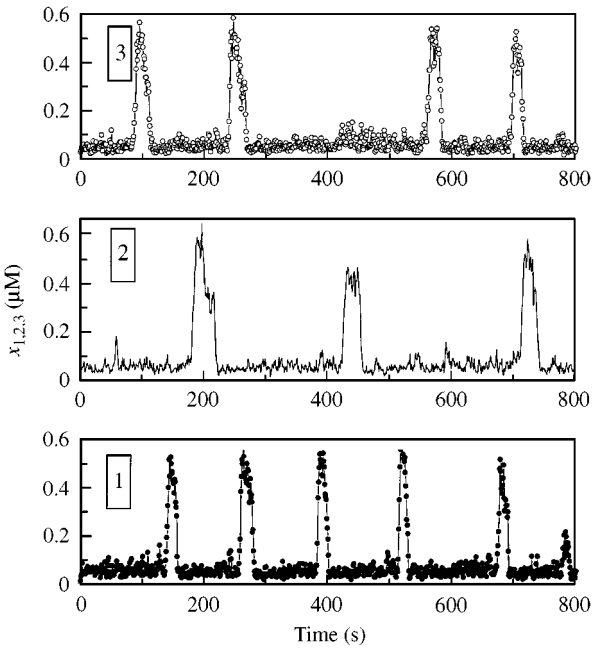

FIG. 6. Evolution of calcium concentrations according to the stochastic version of Höfer's model for three globally stimulated cells, $N = 3$ in eqn (1), in the case of blocked gap junctions: $\gamma = 0\ s^{-1}$. Parameters are as in Table 1 with $P_1 = P_2 = P_3 = 1$ μM, $\beta_1 = \beta_2 = \beta_3 = 0.1$. We have considered that the three cells have different structural parameters: $\rho_1 = 0.025$, $\rho_2 = 0.015$, $\rho_3 = 0.02$. The cell volume is $\Omega = 300\ \mu m^3$. Notice that the three cells exhibit uncorrelated calcium spikes.

$$\frac{\partial y_j}{\partial t} = V_j^{PLC} - V_K \frac{y_j x_j^2}{(K_K + y_j)(x_j^2 + K_d^2)} - V_{PH} \frac{y_j}{K_{PH} + y_j} + D_{IP} \frac{\partial^2 y_j}{\partial s^2}, \qquad (15)$$

where

$$IR_a = \frac{1 - R_j^{des}}{1 + (K_{act}/x_j)^3} \frac{y_j^3}{K_{IP}^3 + y_j^3} \qquad (16)$$

and s is the spatial coordinate.

Note that there is intracellular diffusion of calcium and IP_3 as well as intercellular diffusion of IP_3, with the latter providing the coupling between adjacent cells. Although there is no direct experimental evidence for intercellular IP_3 diffusion, Dupont *et al.* (2000) argue that this is the primary coupling mechanism. The IP_3 diffusion is modeled by assuming that at each boundary

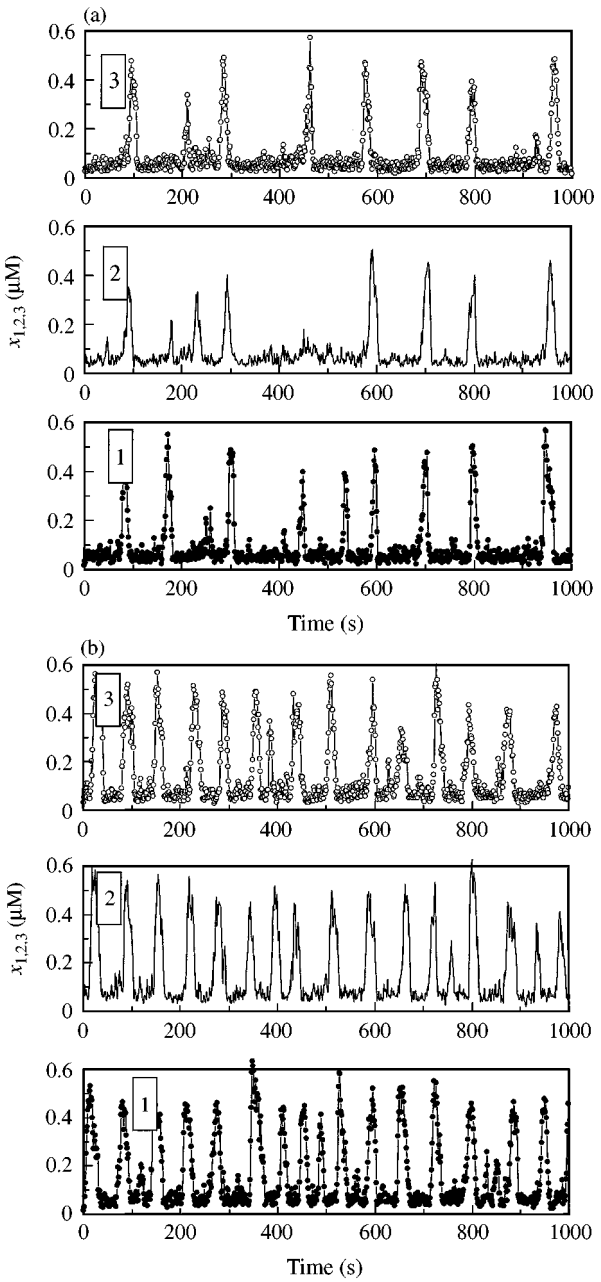

FIG. 7. Results for the low stimulus calcium oscillations in the stochastic version of Höfer's model for three connected cells and $\Omega = 300\ \mu m^3$. The parameters are as in Table 1. In (a) we take $\rho_1 = 0.025$, $\rho_2 = 0.015$, $\rho_3 = 0.02$, $\gamma = 0.07^{-1}$, and apply the same low stimulus to the three cells: $P_1 = P_2 = P_3 = 1\ \mu M$, in (b) we consider structural identical cells $\rho_1 = \rho_2 = \rho_3 = 0.027$, $\gamma = 0.03^{-1}$ and consider a gradient in the IP_3 concentration with $P_1 = 1.2\ \mu M$, $P_2 = 1.1\ \mu M$, $P_3 = 1.0\ \mu M$. Note that while in (a) the three cells become synchronized for times greater than 600 s, in (b) the three cells synchronize only in some time intervals.

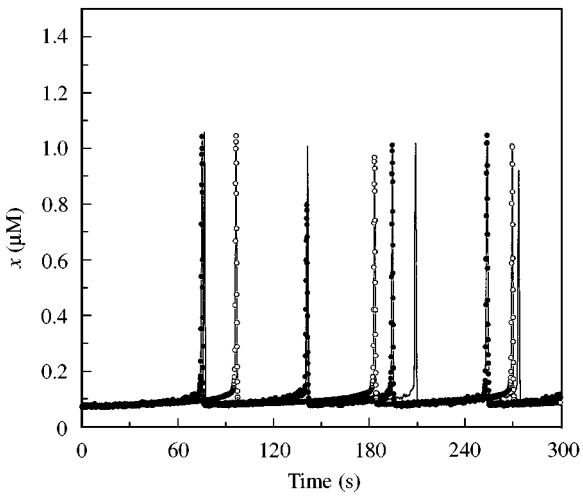

FIG. 8. A study of the dependence of calcium oscillations in one cell on cell volume for the stochastic version of the Dupont *et al.* model, volume values $\Omega = 400$, 2000, 50 000. Notice that, as expected, fluctuations decrease with increasing Ω and that the deterministic limit is already well reproduced by $\Omega = 50\,000$. Initial conditions are resting states corresponding to $V_{PLC} = 6.5 \times 10^{-4}\ \mu M/s$. The rest of parameters are in Table 3 (—•—) Omega = 400; (——) Omega = 2000; (—○—) Omega = 50 000.

between two cells:

$$D_{IP}\frac{\partial y^-}{\partial s} = D_{IP}\frac{\partial y^+}{\partial s} = F_{IP}(y^+ - y^-), \quad (17)$$

where the superscripts " + " and " − " indicate the IP_3 concentration at the right and left limits of the border, respectively. We consider one-dimensional cells 20 μm long, each containing 20 grid points.

We study, using Gillespie's method (Gillespie, 1976), a stochastic version of this model for different cell volumes and for a range of values of the cell–cell permeability. We consider a cell $20\ \mu m \times 20\ \mu m \times 1\ \mu m$ in size (which gives us $\Omega = 400$ for our stochastic simulations), as assumed by Dupont *et al.* (2000). Figure 8 presents the results of our simulation for a single cell for some values of Ω, with the deterministic limit corresponding to large $\Omega = 50\,000$. This shows the dependence of calcium oscillations on the cell volume Ω. The results of our stochastic simulation in this deterministic limit are consistent with that of Dupont *et al.* (2000), as expected. In contrast to the deterministic model where the

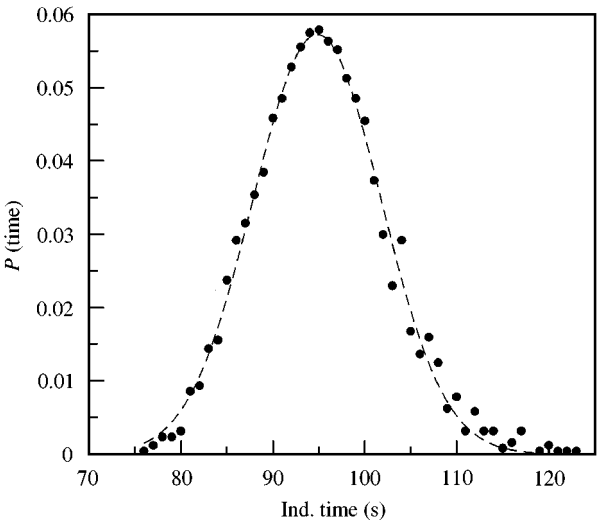

FIG. 9. Distribution of induction times coming from the stochastic version of the Dupont *et al.* model for a single cell with $\Omega = 400$, $V^{PLC} = 2 \times 10^{-3}$ μM/s. Other parameters as in Table 3. The dashed line is a Gaussian fit of mean 95 s and rms 6.9 s.

induction time (latency of cell) depends only on the stimulus strength, we find a distribution of induction times in the stochastic model, due to fluctuations in the calcium concentration. Figure 9 shows the distribution of induction times for one stimulated cell with $V^{PLC} = 2 \times 10^{-3}$ μM/s. As there does not appear to be any systematic experimental study of such a distribution, we have no data to compare our results with. The mean latency time found in our simulation is 95 s. Since the latency time varies with hormonal concentration we cannot make a precise comparison with experiment. However, our result is in reasonable agreement with the experimental values of 30–200 s for the latency times in the literature (Thomas *et al.*, 1991, 1995, 1996). It is also the case that the calcium spikes in these experiments have a width of 20–30 s, which means that it would be difficult to see fluctuations in the central position of the spikes.

For two connected cells we determine the cell–cell permeability following reference (Dupont *et al.*, 2000), such that a doublet of cells, with only one cell doped with stimulant, exhibits calcium oscillations only in the stimulated cell (as has been shown experimentally). Figure 10a presents these data. The results obtained from this stochastic model are in agreement with

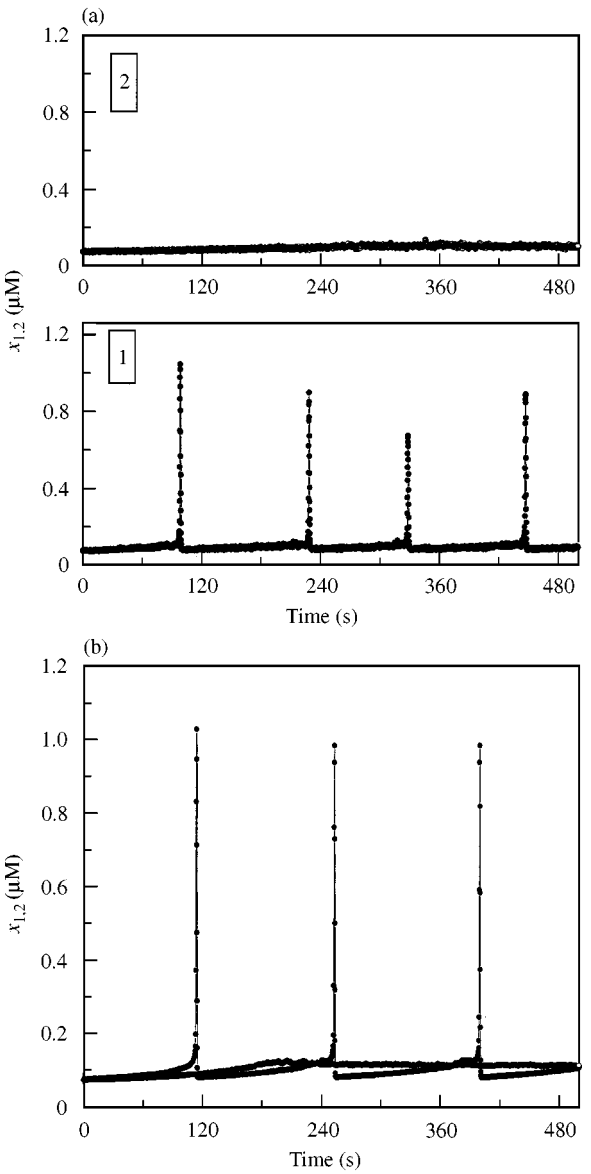

FIG. 10. Calcium oscillations in two connected cells as obtained from the stochastic version of the Dupont *et al.* model. Only the first cell is stimulated. We use this model experiment as a method of adjusting the membrane permeability F_{IP} since it is known that stimulation of just one cell does not produce response in the second cell. (a) Genuine stochastic case with $\Omega = 400$, $F_{IP} = 0.35$, $V_1^{PLC} = 2.5 \times 10^{-3}$ μM/s, $V_2^{PLC} = 6.5 \times 10^{-4}$ μM/s, other parameters as in Table 3. (b) Deterministic limit obtained by taking the large value $\Omega = 50\,000$. Following the parameters used in (Dupont *et al.*, 2000) (Fig. 3c) we set $F_{IP} = 0.88$, $V_1^{PLC} = 2.77 \times 10^{-3}$ μM/s, $V_2^{PLC} = 6.5 \times 10^{-4}$ μM/s and the rest of the parameters as in Table 3 (—•—) 1; (—◦—) 2.

experiment (Dupont *et al.*, 2000), although the cell-to-cell permeability $F_{IP} = 0.35$ μm/s differs somewhat from that in the deterministic model, $F_{IP} = 0.88$ μm/*s* (Dupont *et al.*, 2000). We have to

TABLE 3
Simulation constants for model with intercellular diffusion of IP_3

Parameter	Value
k_+	$25.0\ s^{-1}\ \mu M^{-4}$
k_-	$2.5 \times 10^{-3}\ s^{-1}$
K_{act}	0.34 μM
k_1	$42.0\ s^{-1}\ \mu M^{-1}$
b	10^{-4}
V_{MP}	8.0 μM/s
K_p	0.4 μM
α	0.1
Ca_{tot}	60.0 μM
K_{IP}	1 μM
V_K	7.5×10^{-3} μM/s
V_{PH}	7.5×10^{-2} μM/s
K_K	1 μM
K_{PH}	10 μM
K_d	0.5 μM
D_{Ca}	30 $\mu m^2/s$
D_{IP}	210 $\mu m^2/s$
F_{IP}	0.35 μm/s

use a smaller value for the permeability because noise in the baseline produce spikes in the second, non-stimulated cell if the permeability is larger then 0.35 μm/s. We use $V_1^{PLC} = 2.5 \times 10^{-3}$ μM/s, $V_2^{PLC} = 6.5 \times 10^{-4}$μM/s. We decreased the value of V^{PLC} to obtain agreement with the experimental values of the average induction time. We also find that the stochastic model with the parameters of reference (Dupont *et al.*, 2000) reproduces the deterministic model in the limit of large cell volume. This is to be expected, as in that limit fluctuation effects become negligible. Figure 10b shows the results of the stochastic model in the deterministic limit for the same parameters as in Dupont *et al.* (2000) (permeability $F_{IP} =$ 0.88 μm/s, $V_1^{PLC} = 2.77 \times 10^{-3}$ μM/s, $V_2^{PLC} = 6.5 \times 10^{-4}$μM/s). Another distinguishing feature from the deterministic model is that stochastic effects produce a variation in the spike amplitudes, as was clearly seen in Fig. 8.

Figure 11a shows the result of the simulations for two connected, both stimulated, cells. These cells do not go out of phase as rapidly as in the deterministic model (results not shown).

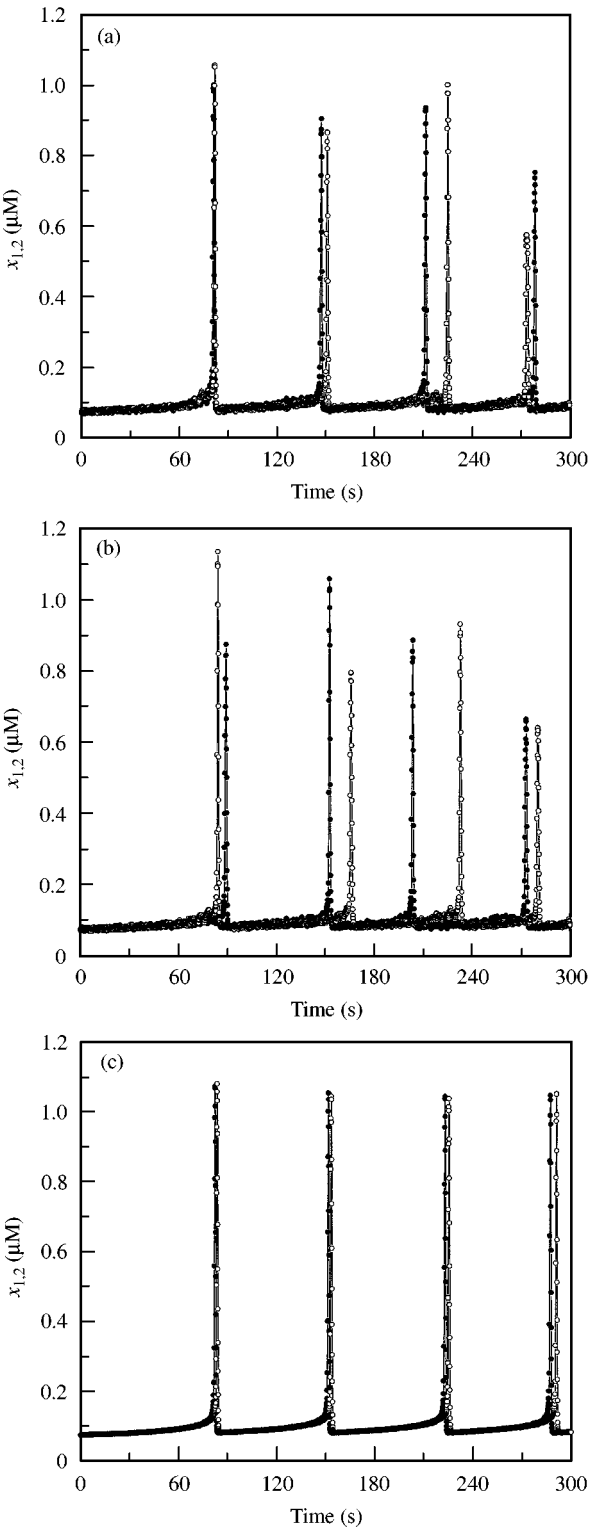

FIG. 11. Calcium oscillations in two connected cells. Both cells are stimulated. (a) and (b) correspond to the genuine stochastic case while (c) is the deterministic limit. Parameters as in Table 3 and (a) $\Omega = 400$, $F_{IP} = 0.35$, $V_1^{PLC} = 2.2 \times 10^{-3}$ μM/s, $V_2^{PLC} = 2.1 \times 10^{-3}$ μM/s; (b) $\Omega =$ 400, $F_{IP} = 0.0$, $V_1^{PLC} = 2.2 \times 10^{-3}$ μM/s, $V_2^{PLC} = 2.1 \times 10^{-3}$ μM/s; (c) $\Omega = 50\,000$ (deterministic limit) and $F_{IP} = 0.88$, $V_1^{PLC} = 2.205 \times 10^{-3}$ μM/s, $V_2^{PLC} = 2.1 \times 10^{-3}$ μM/s, (—•—) 1; (—◦—) 2; to match those used in (Dupont *et al.*, 2000) (Fig. 3d).

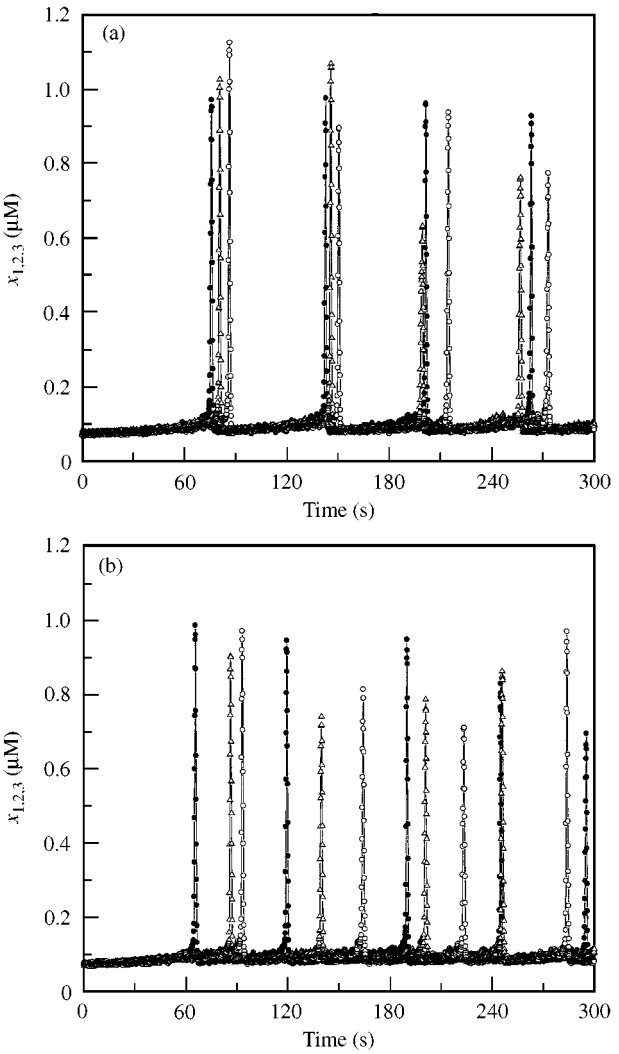

FIG. 12. Study of the effect of gap junction permeability F_{IP} on synchronization of three cells using the stochastic version of the Dupont *et al.* model. Parameters as in Table 3 and $\Omega = 400$, $V_1^{PLC} = 2.3 \times 10^{-3}$ μM/s, $V_2^{PLC} = 2.2 \times 10^{-3}$ μM/s, $V_3^{PLC} = 2.1 \times 10^{-3}$ μM/s. (a) $F_{IP} = 0.35$, (b) $F_{IP} = 0.0$; (—•—) 1; (—△—) 2; (—○—) 3.

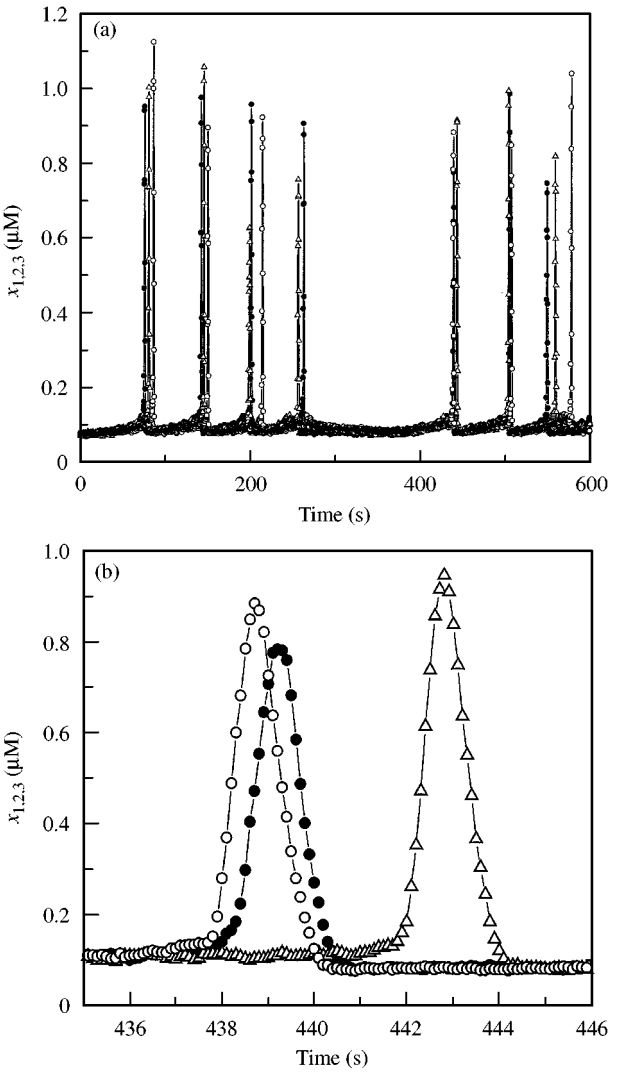

FIG. 13. (a) Numerical experiment using the stochastic version of the Dupont *et al.* model for three connected cells with agonist removal right before third cell spikes at $t = 258$ s. After restoration of agonist at $t = 358$ s third cell spikes first. Parameters the same as for Fig. 12(a). (b) The same as in Fig. 13(a), magnified around $t = 358$ s: (—•—) 1; (—△—) 2; (—○—) 3.

Figure 11b shows two cells with IP_3 diffusion suppressed ($F_{IP} = 0.0$ μm/s). Note that Fig. 11c shows our results in the deterministic limit for large volume, for the same parameters as in Dupont *et al.* (2000).

The experimental results exhibit more synchronization between cells than in this stochastic model. However, the stochastic model yields better agreement with experiment then the deterministic model in terms of the variation in amplitudes and period variations (for $\Omega = 400$). As noted in the introduction, the narrow width of the calcium peaks is a weakness of this model. Also note that in this model the cell with smaller sensitivity can spike first depending on random fluctuations in the second cell (at $\Omega = 400$) than the deterministic model.

For three connected cells we find, in general, the same results as for two connected cells. Fig. 12a and b shows the effect of gap junction permeability on the synchronization of calcium oscillations in three cells. The cells spike in phase for several times, but then gradually lose synchronization. Finally, in Fig. 13, we simulate the effect of washing of agonist at $t = 258$ s just

before the third cell spikes. Washing simulated setting $V_{1,2,3}^{PLC} = 6.5 \times 10^{-4}$ μM/s), its basal level. After restoration of the agonist at $t = 358$ s, the third cell normally spikes first (Fig. 13a) as had happened during the experiment and deterministic simulation (Dupont *et al.*, 2000), but this is not always the case and depends on fluctuations for the stochastic model.

4. Conclusion

We have studied calcium oscillations in connected hepatocytes for two different stochastic models of calcium dynamics. The first model (Höfer, 1999) describes calcium dynamics between the endoplasmic reticulum and cytosol, with diffusion of calcium between connected cells. In the second model (Dupont *et al.*, 2000) connected cells have a gradient in IP_3 sensitivity with diffusion of IP_3 between neighboring cells. Both models are described by a system of nonlinear differential equations. We have solved these two models using a Monte Carlo approach, considering each term in a model as a specific reaction occurring with a certain reaction rate. Our stochastic models are in better agreement with experiment than are the deterministic models. Both stochastic models exhibit baseline fluctuations and variations in peak heights. The baseline fluctuations are somewhat smaller in the second model with diffusion of IP_3 between cells, due to an averaging of calcium concentration over the cell volume, as well as to model characteristics. The drawback of the Dupont *et al.* model is the very narrow width of the calcium spikes. This results in a distribution of latency times with a width of about 15 s which is about the same order as the spike widths observed in experiments. This would make it somewhat difficult to see such a distribution. In addition, the model could be significantly improved by a modification that would yield broader spikes. When compared to the deterministic model, one finds that a smaller permeability coefficient is needed in the stochastic model, since calcium fluctuations on the baseline level give rise to calcium oscillations in the non-stimulated cell if only one cell is stimulated. It would be useful to have experimental results for calcium oscillations on a much longer time scale than is normally presented, since the stochastic model shows that doublets of cells can lose synchronization of calcium oscillations, but can subsequently regain it.

The model (Höfer, 1999) with diffusion of Ca^{2+} between cells reproduces the experimental results for two cells with only one of the cells stimulated. The model reproduces the experimental behavior in which the unstimulated cell does not show calcium oscillations. Also, in accordance with experiments, when the two cells are both globally stimulated, well-coordinated calcium oscillations can be seen in both cells. In the stochastic model, the frequency of final oscillations of coupled cells was slightly smaller than the frequency of the cell with larger frequency oscillations in the doublet (when the cells are not connected by gap junction diffusion). We have found that although this model works quite well for average stimuli strength, the model does not reproduce the observed experimental response of cells at low stimuli with different structural parameters for three connected cells. This is also true when the cells have different IP_3 sensitivity. Instead of a gradual loss of synchronization, cells remain synchronized with a larger period of spiking. They also remain synchronized for gap junctional permeabilities as small as $\gamma = 0.035\ s^{-1}$. With a further decrease of gap junction permeability, the cells initially do not oscillate together, but can subsequently become synchronized. All the results of both deterministic models have been reproduced for their stochastic versions, in the limit of large volume, as should be the case. Finally, we conclude that it is important to take into account stochastic effects in modeling calcium oscillations in connected hepatocytes.

This work was supported in part by NSF Grant number DMR9813409 and the DGES (Spain) projects PB97-0141-C02-01 and BFM2000-1108. We thank K. Prank for bringing this problem to our attention and for helpful discussions. We also wish to acknowledge helpful correspondence with G. Dupont.

REFERENCES

BEZPROZVANNY, I. & EHRLICH, B. E. (1995). The inositol 1,4,5-trisphosphate ($InsP_3$) receptor. *J. Mem. Biol.* **145,** 205–216.

BIRD, G. S. J., OBIE, J. F. & PUTNEY, J. W. (1997). Effect of cytoplasmic Ca^{2+} on (1,4,5) IP_3 formation in vasopressin-activated hepatocytes. *Cell Calcium.* **21,** 253–256.

CHARLES, A. C., NAUS, C.C. G., ZHU, D. G., DIRKSEN, K. E. R. & SANDERSON, D. L. (1992). Intercellular calcium signaling via gap junctions in glioma cells. *J. Cell. Biol.* **118,** 195–201.

COMBETTES, L., TRAN, D., TORDJMANN, T., LAURENT, J., BERTHON, B. & CLARET, M. (1994). Sequential activation of hormone-mediated Ca^{2+} signals in multicellular systems of rat hepatocytes. *Biochem. J.* **304,** 585–594.

DEYOUNG, G. W. & KEIZER, J. (1991). A single-pool inositol 1,4,5-trisphosphate receptor-based model for agonist-stimulated oscillations in Ca^{2+} concentration. *Proc. Natl Acad. Sci. U.S.A.* **89,** 9895–9899.

DUPONT, G. & GOLDBETER, A. (1993). A one-pool model for Ca^{2+} oscillations involving Ca^{2+} and inositol 1,4,5-trisphosphate as co-agonists for Ca^{2+} release. *Cell Calcium* **22,** 311–322.

DUPONT, G., TORDJMANN, Th., CLAIR, C., SWILLENS, St., CLARET, M. & COMBETTES, L. (2000). Mechanism of receptor-oriented intercellular calcium wave propagation in hepatocytes. *FASEB J.* **14,** 279–289.

FALCKE, M., TSIMRING, L. & LEVINE, H. (2000). Stochastic spreading of intracellular Ca^{2+} release. *Phys. Rev. E* **62,** 2636–2643.

GILLESPIE, D. (1976). A general method for numerically simulating the stochastic time evolution of coupled chemical reactions. *J. Comp. Phys.* **22,** 403–434.

GILLESPIE, D. (1977). Exact stochastic simulation of coupled chemical reactions. *J. Phys. Chem.* **81,** 2340–2361.

GOLDBETER, A. (1996). Biochemical Oscillations and Cellular Rhythms. Cambridge University Press, Cambridge.

HANSEN, M., BOITANO, S., DIRKSEN, E. R. & SANDERSON, M. J. (1993). Intercellular calcium signaling induced by extracellular adenosine 5′-trisphosphate and mechanical stimulation in airway epithelial cells. *J. Cell. Sci.* **106,** 995–1004.

HANSEN, M., BOITANO, S., DIRKSEN, E. R., SANDERSON, M. J. (1995). A role for phospholipase C activity but not ryanodine receptors in the initiation and propagation of intercellular calcium waves. *J. Cell Sci.* **106,** 2583–2590.

HÖFER, A. M., CURCI, S., DOBLE, M. A., BROWN, E. M., SOYBEL, E. M. & SOYBEL, D. I. (2000). Intercellular communication mediated by the extracellular calcium-sensing receptor. *Nature Cell Biol.* **2,** 392–398.

HÖFER, Th. (1999). Model of intercellular calcium oscillations in hepatocytes: synchronization of heterogeneous cells. *Biophys. J.* **77,** 1244–1256.

KEIZER, J. & SMITH, G. D. (1998). Spark-to wave transition: salitatory transmission of calcium waves in cardiac myocytes. *Biophys. Chem.* **72,** 87–100.

KEIZER, J., SMITH, G. D., PONCE-DAWSON, S. & PEARSON, J. E. (1998). Saltatory propagation of Ca^{2+} waves by Ca^{2+} sparks. *Biophys. J.* **75,** 595–600.

KRAUS, M., WOLF, B. & WOLF, B. (1996). Crosstalk between cellular morphology and calcium oscillation patterns. *Cell Calcium* **19,** 461–472.

LI, Y. X. & RINZEL, J. (1994). Equations for $InsP_3$ receptor-mediated $[Ca]_i$ oscillations derived from a detailed kinetic model: Hodgkin–Huxley-like formalism. *J. theor. Biol.* **166,** 461–473.

LOESSBERG-STAUFFER, P., ZHAO, H., LUBY-PHELPS, K., MOSS, R. L., STAR, R. A. & MUALLEM, S. (1993). Gap-junction communication modulates $(Ca^{2+})_i$ oscillations and enzyme secretion in pancreatic acini. *J. Biol. Chem.* **268,** 19 769–19 775.

NATHANSON, M., BURGSTAHLER, A., MENNONE, A., FALLON, M., GONZALEZ, G. & SAEZ, J. (1995). Ca^{2+} waves are organized among hepatocytes in the intact organ. *Am. J. Physiol.* **32,** G167–G171.

NATHANSON, M. & BURGSTAHLER, A. (1995). Coordination of hormone-induced calcium signals in isolated rat hepatocyte couplets. Demonstration with confocal microscopy. *Mol. Biol. Cell* **3,** 113–121.

NICHOLSON, B., DERMIETZEL, R., TEPLOW, D., TRAUB, O., WILLECKE, K. & REVEL, J. P. (1987). Two homologous protein components of hepatic gap junctions. *Nature* **329,** 732–734.

PRANK, K., AHLVERS, U., BAUMGARTE, F., MUSMANN, H. G., VON ZUR MUEHLEN, A., SCHOEFL, C. & BRABANT, G. (1998). Stochastic model of intracellular calcium spikes. In: *Meditinische Biometrie* (Guiser, E., Wischnewsky, M. eds) pp 385–388. MMV, Medizin-Verlag, Munchen.

ROBB-GASPERS, L. & THOMAS, A. (1995). Coordination of Ca^{2+} signaling by intercellular propagation of Ca^{2+} waves in the intact liver. *J. Biol. Chem.* **270,** 8102–8107.

SANDERSON, M. J., CHARLES, A. C. & DIRKSEN, E. (1990). Mechanical simulation and intercellular communication increases intracellular Ca^{2+} in epithelial cells. *Cell. Regulat.* **1,** 585–596.

SANDERSON, M. J., CHARLES, A. C., BOITANO, S. & DIRKSEN, E. R. (1994). Mechanisms and function of intercellular calcium signaling. *Mol. Cell. Endocrinol.* **98,** 172–187.

SNEYD, J., WETTON, B., CHARLES, A. & SANDERSON, M. (1995). Intercellular calcium waves mediated by diffusion of inositol trisphosphate: a two0-dimensional model. *Am. J. Physiol.* **268,** C1 537–C1 545.

SNEYD, J., WILKINS, M., STAHONJA, A. & SANDERSON, M. (1998). Calcium waves and oscillations driven by an intercellular gradient of inositol (1,4,5)-trisphosphate. *Biophys. Chem.* **72,** 101–109.

SOMOGYI, R. & STUCKI, W. (1991). Hormone-induced calcium oscillations in liver cells can be explained by a simple one-pool model. *J. Biol. Chem.* **266,** 11 068–11 077.

STUNDZIA, A. B. & LUMSDEN, C. J. (1996). Stochastic simulation of coupled reaction-diffusion processes. *J. Comp. Phys.* **127,** 196–207.

THOMAS, A. P., BIRD, G. S. J., HAJNOCZKY, G., ROBB-GASPERS, L. D. & PUTNEY, J. W. (1996). Spatial and temporal aspects of cellular calcium signaling. *FASEB J.* **10,** 1505–1517.

THOMAS, A. P., RENARD-ROONEY, D. C., HAJNOCZKY, G., ROBB-GASPERS, L. D., LIN, C. & ROONEY, T. A. (1995). Subcellular organization of calcium signaling in hepatocytes and intact liver. *Ciba Foundation Symposia* **188,** 18–35.

THOMAS, A. P., RENARD, D. C., ROONEY, T. (1991). Spatial and temporal organization of calcium signaling in hepatocytes. *Cell Calcium* **12,** 111–126.

TORDJMANN, Th., BERTHON, B., JACQUEMIN, E., CLAIR, C., STELLY, N., GUILLON, G., CLARET, M. & COMBETTES, L. (1998). Receptor-oriented intercellular waves evoked by vasopressin in rat hepatocytes. *EMBO J.* **17,** 4695–4703.

TORDJMANN, Th., BERTHON, B., CLARET, M. & COMBETTES, L. (1997). Coordinated intercellular calcium waves induced by noradrenaline in rat hepatocytes: dual control by gap junction permeability and agonist. *EMBO J.* **16,** 5398–5407.

YULE, D. I., STUENKEL, E. & WILLIAMS, J. A. (1996). Intercellular calcium waves in rat pancreatic acini: mechanism of transmission. *Am. J. Physiol.* **40**, C1285–C1294.